Velocity of second sound and mutual friction in rotating helium II

R. J. Miller, I. H. Lynall, and J. B. Mehl
Physics Department, University of Delaware, Newark, Delaware 19711
(Received 29 August 1977)

The dependence of u_2, the velocity of second sound, on the angular velocity ω has been measured in rotating helium II in the temperature range $1.40 \leq T \leq 2.05$ K. A linear dependence of u_2 on ω was observed for the entire experimental range of angular velocities $\omega \leq 4$ rad/sec. The slopes can be accurately described by the relation $\Delta u_2/u_{20} = -(1/2)B_2\omega/\sigma$, where $\sigma/2\pi$ is the second-sound frequency. The mutual friction parameter B_2 in this relation was previously calculated from experimental values of the parameters B_1 and B_1' by Mehl. Experimental values of B_2 determined from the slopes $\Delta u_2/\Delta\omega$ are in excellent agreement with the calculated values over the entire temperature range $1.40 \leq T \leq 2.05$ K. This agreement provides new support for the correctness of the Hall-Vinen theory of the interaction of second sound with vortex lines. The dependence of the parameter B_1 on second-sound frequency has also been measured. The agreement of the results with the Hall-Vinen theory also provides new support for the detailed correctness of this theory.

I. INTRODUCTION

Experimental and theoretical work on the interaction of second sound with superfluid vortices was first published by Hall and Vinen in 1956.[1] A number of theoretical[2-7] and experimental[8-15] papers have dealt with this subject since then. In recent years, a decrease of u_2, the velocity of second sound, has been observed in rotating helium.[16-19] Lhuillier, Vidal, leRay, and Francois originally discussed this decrease in terms of a coupling between heat currents and counterflow.[20] Later Lhuillier and Vidal[18,21] proposed an explanation of the coupling mechanism based on the theory of Hall and Vinen. An alternate explanation of the dependence of u_2 on rotation, also based on the Hall-Vinen theory, was proposed by Mehl.[18,22]

New measurements of the decrease of u_2 in rotation are presented in this paper.[23] The measurements are in close agreement with the calculation of Mehl and disagree with both the experiments[16-18] and theory[18,20] of the other groups. An explanation of the disagreement between the two experiments is presented later in this paper. Some problems with the theory of Lhuillier *et al.* are also pointed out.

New evidence in support of the theory of Hall and Vinen was also found in measurements of the dependence of the mutual friction parameter B_1 on the second-sound frequency.

The paper is arranged as follows: A review of the theory of Hall and Vinen and the calculations of Mehl is presented in Sec. II. The experimental principle and techniques of data analysis are explained in Secs. III and IV. The apparatus and experimental method are described in Secs. V and VI. Measurements of the velocity of second sound in rotation are presented in Sec. VII, along with discussions of the experimental and theoretical work of the other groups. Measurements of the parameter B_1 and its frequency dependence are presented in Sec. VIII. The paper is concluded with a short summary.

II. INTERACTION OF SECOND SOUND WITH VORTEX LINES

A review of the theory of Hall and Vinen and the calculations of Mehl is presented in this section. Hall and Vinen first described the interaction of second sound with superfluid vortex lines in terms of a force of mutual friction between the normal fluid and superfluid.[1] The force per unit volume $\vec{F}$ is equal to the vortex density $2\omega/\kappa$ times $\vec{f}$, the force per unit length of vortex line. Here $\vec{\omega}$ is the angular velocity and $\kappa = h/m_{He}$ is the quantum of circulation. The force $\vec{f}$ is given by

$$\vec{f} = D\,\vec{v}_{RL} + (D' - \rho_n\kappa)\hat{\omega} \times \vec{v}_{RL} \quad , \tag{1}$$

where $\vec{v}_{RL} = \vec{v}_R - \vec{v}_L$ is the relative velocity of rotons near the lines with respect to the lines, D and D' are proportional to the cross sections for momentum transfer parallel and perpendicular to $\vec{v}_{RL}$, ρ_n is the normal fluid density, and $\hat{\omega}$ is a unit vector along the rotation axis and hence parallel to the vortex lines. For simplicity all velocities are assumed to be perpendicular to $\hat{\omega}$. The force component proportional to $\rho_n\kappa$ is the Iordanskii force.[4] In order to obtain $\vec{F}$ in terms of the macroscopic superfluid and normal fluid velocities $\vec{v}_s$ and $\vec{v}_n$, it is necessary to relate $\vec{v}_R$ and $\vec{v}_L$ to these velocities. The velocities $\vec{v}_s$ and $\vec{v}_n$ are as-

sumed to be average quantities, representing averages over regions containing many vortex lines, while small compared with the wavelength of second sound. The Magnus-effect formula is used to relate $\vec{v}_L$ to $\vec{v}_s$ (Ref. 7):

$$\vec{f} = \rho_s \kappa \hat{\omega} \times (\vec{v}_s - \vec{v}_L) \ , \tag{2}$$

where ρ_s is the superfluid density.

The effects investigated in the present work originate in the relation between $\vec{v}_R$ and $\vec{v}_n$. Let $\vec{v}_R$ be the average roton drift velocity in a region within about one roton-roton mean free path of a vortex line, and $\vec{v}_{n0}$ be the average roton drift velocity far from the line. Hall and Vinen estimated the difference between these velocities by using the model of a wave in a viscous fluid interacting with a solid wire. The result is

$$\vec{v}_{n0} - \vec{v}_R = \vec{f}/E \ , \tag{3}$$

where

$$1/E = [-\ln(\tfrac{1}{2}\lambda L) - 1 - \tfrac{1}{4} i\pi]/4\pi\eta \ . \tag{4}$$

Here L is the roton-roton mean free path, η is the normal fluid viscosity, and λ is proportional to the reciprocal of the viscous penetration length. In terms of the second-sound frequency $\sigma/2\pi$, λ is given by $\lambda = (\rho_n \sigma/\eta)^{1/2}$. The net effects of Eqs. (3) and (4) are (i) the average roton drift velocity near the vortex lines differs from the average roton drift velocity far from the lines by a factor which is typically on the order of $\frac{1}{2}$; this factor depends on the frequency $\sigma/2\pi$; (ii) the imaginary term in Eq. (4) introduces phase shifts which lead to out-of-phase force components.[22] *It is these phase and frequency-dependence effects in Eq. (3) which are investigated in the present work.*

If Eqs. (2) and (3) are used to eliminate $\vec{v}_L$ and $\vec{v}_n$ from Eq. (1), the result can be expressed as a mutual friction force

$$\vec{F} = -\frac{\rho_s \rho_n}{\rho} \omega \left(B_1 \vec{v}_{sn} + \frac{B_2 \dot{\vec{v}}_{sn}}{\sigma} + B_1' \hat{\omega} \times \vec{v}_{sn} + B_2' \hat{\omega} \times \frac{\dot{\vec{v}}_{sn}}{\sigma} \right) \ , \tag{5}$$

where $\vec{v}_{sn} = \vec{v}_s - \vec{v}_{n0}$, $\rho = \rho_s + \rho_n$, and the real part of all complex terms has been taken. The B parameters in Eq. (5) depend on the scattering parameters D and D' and second-sound frequency $\sigma/2\pi$, as well as on the other parameters appearing in Eqs. (1)–(3). Hall and Vinen, who neglected the imaginary term in Eq. (4), expressed $\vec{F}$ in terms of the parameters B and B', which have here been replaced by the complex parameters $B_1 + iB_2$ and $B_1' + iB_2'$. Experimental values of B_1 and B_1' have been used to determine the scattering parameters D and D'. These, in turn, have been used to calculate the parameters B_2 and B_2'.[22]

The parameter B_2 has been measured as a function of temperature in the present work. The results are compared with calculated values. The comparison provides a test of the details and internal consistency of the Hall-Vinen theory.

The relation between $\vec{v}_R$ and $\vec{v}_{n0}$ leads to a weak dependence of all the mutual friction parameters on the second-sound frequency. For example, doubling a typical second-sound frequency at 1.65 K will increase B_1 by 2.5%. This parameter has been precisely measured in this work. The results have been used to compare the experimental frequency dependence with theory. This is an additional test of the correctness of the Hall-Vinen theory.

The primed parameters in Eq. (5) are unimportant in the present work and will be omitted in the following discussion. If $\vec{F}$ is included in the two-fluid hydrodynamic equations, the following wave equation for second sound is obtained:

$$\ddot{\vec{q}} = u_2^2 \nabla\nabla \cdot \vec{q} + (\rho/\rho_s\rho_n) \dot{\vec{F}} \ , \tag{6}$$

where $\vec{q} = \vec{v}_s - \vec{v}_n$. It is important to be precise about the definition of $\vec{v}_n$ in the hydrodynamic equations. It is equal to the average drift velocity of all the rotons, and hence differs from $\vec{v}_{n0}$ by a small amount, since the rotons near the vortex lines have a different average drift velocity. The difference depends on the number of vortex lines and hence on ω. In the following only effects linear in ω are considered, hence the difference between $\vec{v}_n$ and $\vec{v}_{n0}$ in the expression for $\vec{F}$ [Eq. (5)] can be neglected, and Eqs. (5) and (6) can be combined to give

$$\ddot{\vec{q}} = u_2^2 \nabla\nabla \cdot \vec{q} - B_1 \omega \dot{\vec{q}} - B_2 \omega \ddot{\vec{q}}/\sigma \ . \tag{7}$$

The effects of the mutual-friction force terms in Eq. (7) can be easily seen by considering a one-dimensional solution $q = q_0 \exp[i(kx - \omega t) - \alpha x]$. Substitution of this form into Eq. (7) leads to

$$u_2(\omega, \sigma) = \omega/k \simeq u_2(1 - B_2\omega/2\sigma) \tag{8}$$

and

$$\alpha \simeq B_1 \omega/2u_2 \tag{9}$$

for the usual experimental conditions $\alpha \ll k$, $B_2\omega/\sigma \ll 1$. Equation (8) states that the velocity of second sound in rotating helium is reduced by a fraction $B_2\omega/(2\sigma)$. This equation accurately described the results of Lynall and Mehl[19] at 1.65 K, where $B_2 \simeq 0.06$. The attenuative effect of the parameter B_1 is shown in Eq. (9).

III. EXPERIMENTAL PRINCIPLE

Measurements of the normal-mode frequencies of cylindrical resonators were used to determine the de-

crease of u_2 in rotation and the associated mutual-friction parameter B_2. Measurements of the resonance linewidths were used to determine the parameter B_1 and its dependence on the second-sound frequency. Standing waves were excited using carbon-film transducers on the cylinder walls. The temperature oscillations for these modes are given by

$$T' \propto J_s(k_{ns}r)e^{\pm is\theta} \ , \tag{10}$$

where $J_s(z)$ is the s-order Bessel function. The boundary condition at the cylinder wall, $dJ_s(z)/dz = 0$ at $z = k_{ns}a$, determines the values of k_{ns} and the resonance frequencies $\sigma_{ns} = k_{ns}u_2$. Here a is the cylinder radius. Modes with a component of $\bar{v}_{sn}$ parallel to the cylinder walls are being neglected. The effects of mutual friction [Eq. (5)] and the Coriolis force on the normal-mode frequencies are given by[22]

$$\delta\sigma_{ns} = \tfrac{1}{2}(iB_1 - B_2)\omega \mp [iB_2' - (2 - B_1')] \times (k_{ns}^2a^2 - s^2)^{-1}s\omega \ . \tag{11}$$

The present work was restricted to $s = 0$ modes, for which the only effects are an increase in losses proportional to $\frac{1}{2}B_1\omega$ and a decrease in the resonance frequencies by $-\frac{1}{2}B_2\omega$, in agreement with Eqs. (8) and (9).

For typical experimental conditions $B_2 \simeq 0.06$, $\omega \simeq 2$ rad/sec, and $\sigma/2\pi \simeq 1000$ Hz, the fractional decrease in the resonance frequency is on the order of 10 ppm. A study of the effect thus requires measurement of the resonance frequencies to a few ppm. Since typical resonance Q's were in the range 10^3–10^4, it was necessary to fit experimental measurements to a theoretical resonance formula to determine the resonance frequencies with sufficient accuracy. This method of analysis is described in Sec. IV.

IV. ANALYSIS OF STANDING-WAVE MEASUREMENTS

A. General

When a second-sound resonator is excited by driving an emitter transducer at a frequency near one of the resonance frequencies σ_0, the amplitude of the temperature oscillations can be described by the Lorentzian formula

$$A = a_0[\gamma + i(\sigma - \sigma_0)]^{-1} \ , \tag{12}$$

where a_0 is proportional to the emitter power and γ is the resonance half-width. Note that a_0/γ is the amplitude at resonance. In general there will be a background signal owing to weak excitation of other modes. If the frequencies of the other modes are well separated from σ_0 the background will be approximately constant, and the total signal can be described by

$$A = a_0[\gamma + i(\sigma - \sigma_0)]^{-1} + b_1 + ib_2 \ . \tag{13}$$

Electrical crosstalk at the second-sound frequency will also contribute to the background. In the present work the background was typically in the range of 0.1%–1% of the maximum signal. It is therefore sufficient to consider only the first-order effect of b_1 and b_2. It is easy to show that the maximum of $|A|$ is shifted from σ_0 to $\sigma_0 + \Delta\sigma$, where

$$\Delta\sigma = -\gamma^2 b_2/a_0 \ . \tag{14}$$

That is, the maximum is shifted by a fraction $(\gamma b_2/a_0)$ of the half-width γ. This fraction is the ratio of the out-of-phase background b_2 to the maximum signal (a_0/γ). Thus in this work $\Delta\sigma$ may be as large as 1% of $\gamma = \sigma_0/(2Q)$. With a Q of 10^3, the correction is 5 ppm, which is significant compared with the effect of interest.

B. Need for a background correction

Consideration of the effect of background in rotation shows that a background correction must be made. The effect of mutual friction on the resonance widths for the $s = 0$ modes is given by[13]

$$\gamma = \gamma_0 + \tfrac{1}{2}B_1\omega \ , \tag{15}$$

where γ_0 is the half-width at rest. The total frequency shift in rotation is found by using Eq. (15) in Eq. (14) and adding the term $(-\frac{1}{2}B_2\omega)$ from Eq. (11), giving

$$\Delta\sigma = -b_2\gamma_0^2/a_0 - \tfrac{1}{2}[B_2 + (b_2\gamma_0/a_0)B_1]\omega - \tfrac{1}{4}(b_2/a_0)B_1^2\omega^2 \ . \tag{16}$$

Thus, for sufficiently small ω, $\Delta\sigma$ will be linear in ω, but the slope will be shifted from $(-\frac{1}{2}B_2)$. The importance of the correction can be estimated by noting that in the present work $(b_2\gamma_0/a_0)$ may be as large as 1%. Since B_2 is on the order of 5% of B_1, failure to correct for background can lead to significant errors in an experimental determination of the parameter B_2.

At higher angular velocities the quadratic term in Eq. (16) becomes important. The effect of this term is evident in the data of Vidal *et al.*,[16,18] and accounts for the large values of $-\Delta u_2/\omega^2$ reported earlier by that group.[17]

C. Determination of the resonance parameters

It is most convenient to eliminate the effect of background by fitting raw data directly to the absolute value of Eq. (13). This is a nonlinear problem. However, for the small background levels found in this work, it was possible to linearize Eq. (13) and to simplify the fitting. Equation (13) can be rearranged to give, to first order in b_1 and b_2,

$$|A|^{-2} = c_0 + c_1\sigma + c_2\sigma^2 + c_3\sigma^3 \ , \tag{17}$$

where

$$\begin{aligned} c_0 &= a_0^{-2}(\gamma^2 + \sigma_0^2)g \ , \\ c_1 &= a_0^{-2}[-2\sigma_0 g + (\gamma^2 + \sigma_0^2)(2b_2/a_0)] \ , \\ c_2 &= a_0^{-2}(-4b_2\sigma_0/a_0 + g) \ , \\ c_3 &= a_0^{-2}(2b_2/a_0) \ , \end{aligned} \tag{18}$$

and

$$g = 1 - 2(b_1\gamma/a_0) - 2(b_2\sigma_0/a_0) \ .$$

These relations can be solved to give the resonance parameters

$$\sigma_0 = -[\tfrac{1}{2}(c_1c_2 - c_0c_3) - 4c_3\sigma_0^2 - 4c_3^2\sigma_0^3] \times (c_2^2 + c_1c_3)^{-1} \ , \tag{19}$$

$$\gamma^2 = c_0(c_2 + 2\sigma_0 c_3)^{-1} - \sigma_0^2 \ . \tag{20}$$

In this work the coefficients $\{c_j\}$ were determined by fitting data $\{A_i, \sigma_i\}$ to Eq. (17). The data were weighted to correspond to a uniform uncertainty in the A_i. About 12 points in the approximate range $\sigma_0 \pm \gamma$ were used. Then σ_0 and γ were calculated from Eqs. (19) and (20). Tests with simulated data show that this method of analysis gives correct values of σ_0 to better than 0.5 ppm as long as b_1 and b_2 are less than 5% of the maximum amplitude, and the resonator Q is greater than 10^3. These conditions are far more severe than the worst experimental case in this work.

V. APPARATUS

A. General

The second-sound resonator was suspended from stainless-steel tubes which extended into the helium Dewar from a turntable at the top of the Dewar system. The resonator was protected from bath turbulence by a brass enclosure. Small holes at the top of the enclosure insured thermal contact between the bath and the resonator. The entire enclosure and support tubes rotated with the turntable. The turntable was supported by a roller bearing. A Teflon ring backed with an O-ring was used for the vacuum seal. Low-level electronics and battery power were rotated with the turntable. Electrical connections to the rotating system were made though a rotary transformer.[24] The turntable was driven through a variable-speed transmission.[25] The rate of rotation was determined electronically by measuring the frequency of a square wave from a shaft-angle encoder coupled to the rotating system. Long term stability of the rotation rate was typically 0.1%.

B. Second-sound resonators

Two cylindrical resonators were used. The resonators were constructed from precision-bore glass (borosilicate) with the cylinder ends ground flat and parallel to the sides. The inner diameters were 3.81 and 5.08 cm. Both cylinders had lengths of 3.81 cm. Eight uniformly spaced slits were cut in the glass at each end of the cylinders. The slits provided a path for electrical leads and for thermal counterflow. The end caps were machined from boron nitride. With the end caps in place, the exposed area of each slit was approximately 0.9 mm^2.

Carbon-film transducers were prepared by spraying a colloidal suspension of carbon[26] on the masked inner walls of the cylinders. Eight uniformly spaced films were applied to each cylinder, with strips of conductive silver paint used for electrical contacts at each end of the cylinder. The carbon-film widths were 1.27 and 1.905 cm for the 3.81- and 5.08-cm resonators, respectively. The films ran nearly the full length of the cylinders. Fine stranded electrical leads were passed through each slit, fanned out, and covered with silver paint to ensure electrical contact with the corresponding films.

The resistances of the individual films are $\sim$1 kΩ at room temperature and $\sim$3 kΩ at 2.0 K, with a temperature coefficient of resistivity $R^{-1}(dR/dT)$ of about 0.15 K^{-1} near 2 K. Four alternately-spaced films were driven in parallel as an emitter. One of the remaining films was biased with a steady current and used as a detector.

C. Temperature control and measurement

A conventional mechanical pumping system was used for rough temperature control. Primary temperature measurements were made by means of helium vapor-pressure measurements with an oil manometer. Resistance thermometry was used for more precise temperature measurements and for fine temperature control.

A doped-germanium thermometer was mounted in the helium bath at the same height as the resonator. Its resistance varied from about 15 kΩ at 2.2 K to about 100 kΩ at 1.4 K. The resistance was measured with a Wheatstone bridge operated at 33 Hz. A lock-in amplifier was used as a null detector and to provide a corrective signal for temperature regulation. The thermometer power was limited to less than 10^{-9} W to minimize self-heating. The corresponding bridge sensitivity is about 1 μK. The regulator was capable of holding drifts to a few μK per day.

Although thermometers were not permanently mounted inside the resonators, a special experiment was performed to ensure that the temperature inside the resonators did not drift when the system was ro-

tated or when power was dissipated in the transducers. A carbon-resistance thermometer was mounted inside one resonator and monitored by a bridge on the rotating table. The sensitivity of this bridge was also about 1 μK. When the system was rotated at 4 rad/sec and the carbon films were heated at typical levels no temperature shifts could be detected.

D. Second-sound electronics

A frequency synthesizer[27] was used to provide a drive signal with high amplitude and frequency stability. The drive signal was passed through one channel of the rotary transformer and applied to four carbon films connected in parallel. The heating of the films generates second sound at twice the synthesizer frequency. One of the remaining carbon films was biased by connecting it to a battery through a large fixed resistor. Resistance oscillations at the second-sound frequency were detected by observing the ac voltage across the detector film. This signal was amplified in the rotating system and passed through a second channel of the rotary transformer to the stationary electronics. A vector lock-in amplifier was used for measuring the signal. The output of the lock-in was measured with a digital voltmeter. With a 3-sec time constant, it was typically possible to measure the second sound signal with a precision of about 0.1%.

Note that with this method of generation and detection any electrical crosstalk at the drive frequency will not be detected as second sound unless there is harmonic generation in the amplifier chain. The danger of this was in any case minimized since, for the film geometry used here, electrostatic coupling between the films was extremely low. The measured crosstalk (at the drive frequency) was less than 0.05% of A_0. In addition, the output of the synthesizer contained less than 0.03% second harmonic.

VI. EXPERIMENTAL METHOD

A. Measurement sequence

Measurements were made at fixed temperatures. After cooling and regulating at a fixed temperature, a preliminary experiment was carried out to insure that the second-sound amplitude was low enough to avoid nonlinear effects. A safe level was determined by plotting the second-sound amplitude at resonance versus the drive power. A departure from linearity identified a critical power which was typically about 4 mW. All subsequent measurements were taken at a lower power level. The detector power was always kept at a level low compared with that of the emitter films.

The remaining measurements at the fixed temperature were made to determine the resonance parameters σ_0 and γ for one or more resonator modes at rest and at several angular velocities. Normally a set of measurements at rest was followed by two or three sets at different angular velocities, then another set at rest, and so on until four or five rest sets and eight to ten rotation sets were obtained. About half the rotation sets were taken with clockwise rotation and the remainder with counterclockwise rotation.

Following each change in the angular velocity, a delay of 30 min was allowed to ensure equilibrium. This time interval was chosen conservatively; experimental checks indicate that a 10-min delay would be sufficient. Following the delay a set of approximately 12 measurements $\{A_i, \sigma_i\}$ was taken. The frequencies were spread over the approximate range $\sigma_0 \pm \gamma$, with approximately uniform spacing. The order of the measurements was randomized. In most cases, this set of measurements was immediately followed by another set using one of the other modes of the resonator.

The temperature was continuously recorded during experimentation and the level of the helium bath was recorded before and after each set of measurements. These data were used to correct the resonance frequencies for small temperature shifts and for the variation of u_2 with pressure.

B. Data analysis

Each set of measurements $\{A_i, \sigma_i\}$ was fitted to the theoretical resonance formula (17) as described in Sec. IV. The fitting provided values of the resonance frequency σ_0, the resonance half-width γ, the maximum amplitude $A_0 = a_0/\gamma$, the fractional out-of-phase background b_2/A_0, and χ^2, the sum of the squared residuals. Typically, the rms residual was 0.05% of A_0 and b_2 was less than 1% of A_0. When the data were divided into two six-point subsets and each set was analyzed separately, the values of σ_0 typically agreed within 1 ppm.

When necessary, the resonance frequencies were corrected for any temperature drifts observed on the chart recorder which monitored the temperature. Since u_2 has a maximum at 1.64 K, these corrections were only necessary at the temperature extremes, and then only infrequently. The magnitude of the corrections seldom exceeded 1 ppm.

Since u_2 is pressure dependent, it was necessary to correct the resonance frequencies for changes in the helium bath level. A set of measurements on a single resonance curve could be taken in less than 15 min. During this time interval the helium bath dropped on the order of 0.25 cm. Thus, since $u_2^{-1}\, du_2/dh$ is on the order of 2-ppm/cm He, σ_0 would drift by no more than about 0.5 ppm during a set of measurements. This drift is negligible and it was not necessary to correct individual measurements. However, it was

necessary to correct for the greater changes in level which occurred between measurements at different angular velocities. It was convenient to combine this correction with the determination of the parameter B_2. The resonance frequencies were fitted to

$$\sigma_0(\omega,h) = \sigma_0(0,0) + u_2^{-1}\left(\frac{du_2}{dh}\right)h - \tfrac{1}{2}B_2\omega \quad . \qquad (21)$$

As a check, the coefficient $u_2^{-1}\, du_2/dh$ was also determined from a separate fit to the $\sigma_0(0,h)$ data. No significant differences between the two values of the coefficient were ever found.

The slopes $u_2^{-1}\, du_2/dh$ determined from these fits are shown in Fig. 1. For comparison, slopes determined from the second sound velocity data of Heiserman *et al.*[28] are shown as a solid line. (Pressure increments on the order of 1 atm were used by Heiserman *et al.*, while the maximum pressure difference in this work was about 3×10^{-4} atm.) Some of the lack of reproducibility in the data of Fig. 1 may be due to small thermometry drifts, which would be corrected to first order in the fit of Eq. (21).

During a normal sequence of measurements at a fixed temperature, the helium bath level dropped by approximately 20 cm. Hence the maximum correction was on the order of 40 ppm, comparable with the magnitude of the decrease described by the B_2 term. The uncertainty of the correction estimated from the quality of the fit to Eq. (21) was typically on the order of 1 ppm.

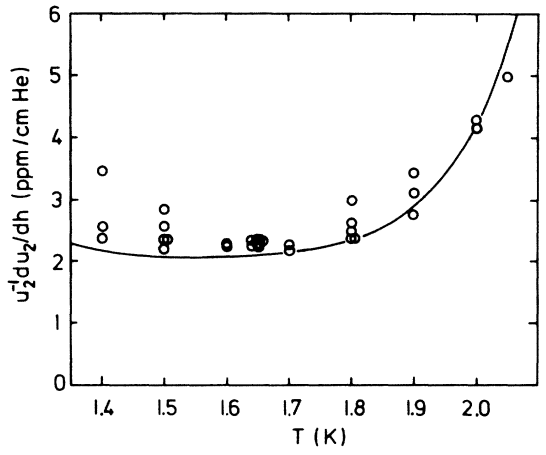

FIG. 1. Fractional dependence of the second-sound velocity on pressure $u_2^{-1}\, du_2/dh$ as a function of temperature. The points were determined from fits to Eq. (21) as explained in the text. Multiple points at a fixed temperature correspond to different second-sound frequencies. The solid line is calculated from the $u_2(p,T)$ data of Heiserman *et al.* (Ref. 28).

VII. VELOCITY OF SECOND SOUND IN ROTATING HELIUM

A. Results

Figure 2 shows the dependence of the resonance frequencies σ_0 on the angular velocity ω at 1.4 K. The data were taken with the 10 mode of the 5.08-cm resonator, and the 10 and 20 modes of the 3.81-cm resonator. Some of the frequencies in Fig. 2 have been corrected for small temperature drifts. The maximum such correction was 0.8 ppm. The frequencies have also been corrected for bath level using the slopes determined by fitting to Eq. (21) as explained above. The frequencies thus corrected are expected to be described by $\Delta\sigma_0(\omega) = -\frac{1}{2}B_2\omega$. The straight lines in Fig. 2 are those determined by the fits to Eq. (21). The slopes correspond to $B_2 = 0.0450$, 0.0445, and 0.0483, respectively. Thus the slopes are approximately the same, in agreement with Eqs. (8) and (11), although the values of $\sigma_0(\omega = 0)$ vary by more than a factor of 2. (The total variation of the parameter B_2 with frequency is on the order of 1% for this range of frequencies and would not be observable.)

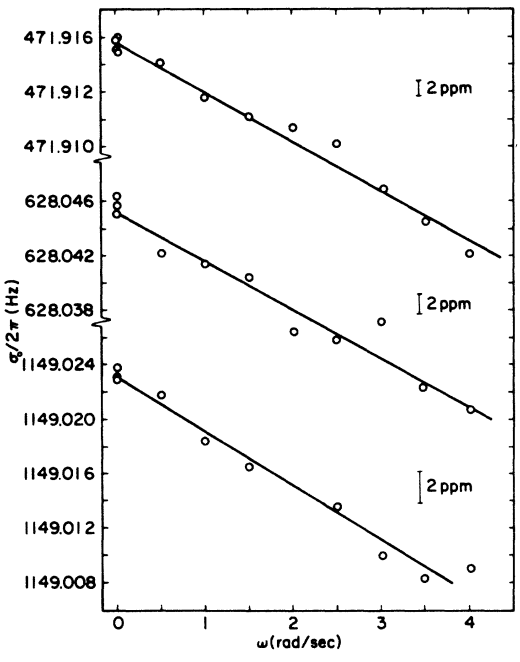

FIG. 2. Second-sound resonance frequencies $\sigma_0/2\pi$ as functions of angular velocity at 1.40 K. The upper data were taken with the 10 mode of the 5.08-cm resonator, and the center and lower data with the 10 and 20 modes of the 3.81-cm resonator, respectively. The frequencies have been corrected for bath level as explained in the text. The linear dependence on ω is in agreement with Eqs. (8) and (11).

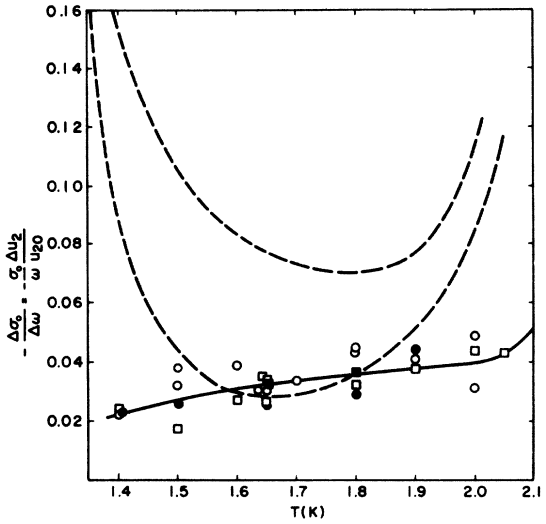

FIG. 3. Slopes $\Delta\sigma_0/\Delta\omega$ determined from linear fits to data similar to those in Fig. 2, vs T. The open and closed symbols correspond to the 3.81- and 5.08-cm resonators, respectively. The circles correspond to the 10 modes, and the squares to the 20 modes. Typical resonator properties are given in Table I. The solid line is the theoretical prediction Eq. (8) with values of B_2 from Ref. 22. The dashed lines enclose the region of similar data from Ref. 18. An explanation of the difference between the two sets of data is given in the text.

Similar measurements were made at other temperatures, using the 10, 20, and 30 modes of the resonators. Because of the relatively high background for the 30 mode, the data obtained using these modes were unreliable and are not reported here. Data taken with the 10 and 20 modes were generally similar to those shown in Fig. 2. A set of data taken with one mode at one temperature normally included approximately the same amount of data as in the cases shown in Fig. 2. In all cases the plots of $\sigma_0(\omega)$ vs ω were linear, and the average deviation of the points from the best linear fit about 1 ppm. The slopes $-\Delta\sigma_0/\Delta\omega = -(\sigma_0/\omega)(\Delta u_2/u_{20})$ are shown in Fig. 3. The different symbols distinguish between the different modes and resonators. The frequencies σ_0 and resonance widths γ_0 for some typical temperatures are listed in Table I. The solid line in Fig. 3 represents the theoretical slope $\frac{1}{2}B_2$. The values of B_2 were calculated as explained in Sec. II.[22] Although there is considerable scatter, the experimental slopes in Fig. 3 are in good agreement with the theoretical slope.

In order to make a closer comparison, the experimental slopes at each temperature were averaged and used to determine experimental values of the mutual friction parameter B_2 These average values are compared with the calculated curve in Fig. 4. The close agreement shows that the decrease of u_2 in rotation can be completely accounted for by the extra term in the expression for the force of mutual friction (5), and provides new support for the details of the Hall-Vinen theory.

The dotted lines in Fig. 3 define a region bounding the results of Vidal and Lhuillier[18] (VL). The disagreement between these data and those determined in the present work may be explained by referring to Eq. (16). VL determined values of the resonance frequency of a rotating rectangular resonator using a "resonance-circle" technique. It is easy to show that background will displace the circles by $(b_1 + ib_2)$ in the complex plane without affecting the shape or diameters of the circles. VL determined values of σ_0 by finding the frequency which corresponded to the intersection of the circle and a diameter which passes through the center of the circle and the point $(b_1 + ib_2)$. This point actually

TABLE I. Selected resonator properties.

Resonator diameter (cm)	Mode	Temperature (K)	Resonance frequency $\sigma_0/2\pi$ (Hz)	Resonance half-width $\gamma_0/2\pi$ (Hz)	$Q = \sigma_0/2\gamma_0$
3.81	10	1.4	628	0.127	2470
		1.65	654	0.0746	4380
		2.0	534	0.0496	5380
	20	1.4	1149	0.170	3380
		1.65	1196	0.110	5440
		2.0	978	0.0586	8340
5.08	10	1.4	472	0.139	1700
		1.65	491	0.0980	2510
		2.0	399	0.0556	3590
	20	1.65	899	0.0940	4780

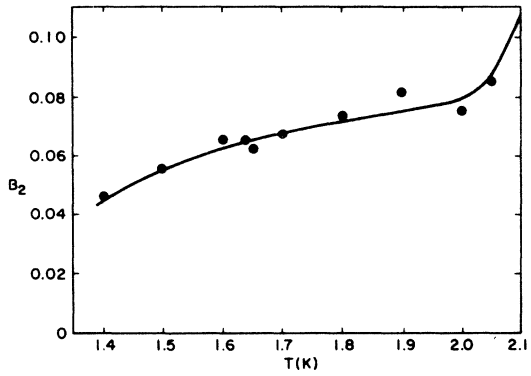

FIG. 4. Mutual friction parameter B_2 vs T. The points were determined by averaging the data in Fig. 3 at each temperature. The solid line was calculated by Mehl (Ref. 22), using experimental values of the parameters B_1 and B_1'. The agreement supports the internal consistency and details of the Hall-Vinen theory.

corresponds to the frequency given by Eq. (16). VL state that the electronic pickup in their experiment was on the order of 5% of the maximum signal. Since they generated second sound at the oscillator frequency using a biased emitter, this pickup was a steady background, which in turn led to a spurious change of σ_0 in rotation. According to Eq. (16), the background will shift the slope of the $\sigma_0(\omega)$ curve at 1.65 K by approximately $\frac{1}{2}(0.05)B_1 \simeq 0.03$, which is approximately the correct magnitude to account for the difference between the two sets of data in Fig. 3. Moreover, Eq. (16) predicts the quadratic contribution to $\sigma_0(\omega)$ observed by Vidal *et al.*[16,18] The sign of the quadratic effect shows that b_2 was positive in their experiment, and hence that the coefficient of the linear term in Eq. (16) will be larger than $\frac{1}{2}B_2$, in agreement with Fig. 3. The difference between the two sets of data in Fig. 3 is greatest at the extremes of temperature. Much of this temperature dependence can be accounted for by the temperature dependence of B_1. Precise background measurements would be necessary to account for the exact dependence. Earlier, Vidal *et al.*[17] reported a quadratic dependence of σ_0 on ω. The temperature dependence of their values of $\Delta u_2/(\omega^2)$ is also qualitatively similar to that of the B_1^2 term in Eq. (16).

B. Experimental checks

Various checks were made to insure that the observed decrease of u_2 in rotation did not arise from spurious sources. These checks are summarized below.

(i) As explained in Sec. V C, a thermometer was mounted in one of the resonators in a special experiment. Within the sensitivity of ~ 1 μK, the temperature inside the resonator did not shift when the apparatus was rotated at angular velocities up to 4 rad/sec and the carbon films were heated at typical levels. Thus temperature shifts in the resonator cannot account for changes of u_2 of more than about 1 ppm.

(ii) As an auxiliary check on temperature effects, a set of carbon film transducers was mounted on one of the resonator endcaps. These were used for generating and detecting second sound in the $\hat{\omega}$ direction. Resonance measurements were made at 1.4, 1.65, and 1.9 K, at rest and in rotation. While there was considerable scatter in these measurements, the shift of u_2 was in all cases less than 10% of the expected value for horizontally propagating second sound at the same frequency. In addition there were no changes in the resonance linewidths greater than 5% of the expected values for horizontal propagation.

(iii) Geometric imperfections in the resonator could in principle give rise to a temperature distribution which contains, in addition to a strongly excited $n0$ state, a mixture of the ns states [cf. Eq. (10)]. The frequencies of the $s \neq 0$ states are shifted by rotation as described by the $(2 - B_1')$ term in Eq. (11). If such a mixture is taken as the "unperturbed" state, and the effect of Eq. (5) is calculated using perturbation theory, the predicted frequency shift will contain terms proportional to the $(2 - B_1')$ term in Eq. (11) and the coefficients of $J_1(k_{ns}r)$ in the expansion of the unperturbed state. The sign of such shifts reverses with reversal of $\bar{\omega}$, however. Measurements of $\sigma_0(\omega)$ were made with both clockwise and counterclockwise rotation. The absence of a consistent difference between measurements taken in the two directions rules out the possibility of a significant contribution from geometric perturbations.

C. Discussion

The experimental results reported above show that the decrease of u_2 in rotating helium can be completely accounted for by the Hall-Vinen theory, provided that phase effects in the velocity perturbation [Eqs. (3) and (4)] are included in the calculation of the force of mutual friction. A different theoretical approach was taken by Vidal, Lhuillier, and colleagues,[18,20,21] who interpreted their measurements of the decrease of u_2 in rotation and in heat currents in terms of a thermodynamic coupling between the force of mutual friction and heat currents. They also constructed a model based on the Hall-Vinen theory to explain the coupling. There are difficulties with both parts of this approach.

It is first important to note that the effects included in the B_2 term of Eq. (5) are intrinsically ac effects; the theoretical basis of Eqs. (3) and (4) is only valid

for sufficiently high frequencies. It is unclear whether there will be an effect at zero frequency, as is assumed in the thermodynamic approach. A further possible source of difficulty is the use of the Onsager reciprocity principle in the thermodynamic theory. This principle only applies to Markoffian systems.[29] It is not clear whether it applies to the system of oscillating vortices and second sound. It is worth considering an analogy with electrical circuits. The component of mutual friction proportional to B_1 is analogous to electrical resistance, while the B_2 component is analogous to inductance. While the Onsager principle applies to complex circuits containing only resistances, it is not applicable to systems containing inductances or capacitances.[29]

The model of vortex motion introduced by Vidal and Lhuillier[18,21] includes three effects: an inertial force on the vortices which has some similarity to the B_2 term in Eq. (5), thermal forces on the vortices, and entropy drag by the moving vortices. The latter two effects are associated with roton drag by the vortices. While it is correct that entropy is transported by the vortices with a local velocity which differs from $\vec{v}_n$, this effect is already included in the entropy conservation equation with a properly defined macroscopically averaged $\vec{v}_n$. Similarly, the thermal force is included in the fountain effect term in the hydrodynamic equations. Stated in another way, if the entropy drag by moving vortices and thermal forces on vortices are to be explicitly included in the equations of motion, for consistency it is also necessary to explicitly include the corresponding rate of change of momentum of the dragged rotons in the $p_n\dot{\vec{v}}_n$ term. Thus the only contribution to Δu_2 which is linear in ω is that of the B_2 term in Eq. (5). (The discussion in Sec. II with respect to the difference between $\vec{v}_{n0}$ and $\vec{v}_n$ is relevant to this point.)

VIII. DEPENDENCE OF MUTUAL FRICTION ON SECOND-SOUND FREQUENCY

Owing to the frequency dependence of the roton-drift-velocity perturbation [Eqs. (3) and (4)], all the mutual friction parameters are frequency dependent. The parameter B_1 is most easily measurable. In this section, measurements of B_1 which are sufficiently sensitive to show the dependence on frequency are presented.

As previously described, the fits to the $\{A_i, \sigma_i\}$ data yielded values of the resonance halfwidth $\gamma(\omega)$. These in turn were fitted to Eq. (15) to determine the parameters γ_0 and B_1. Typical values of γ_0 are given in Table I. (The values of γ_0 determined from fitting did not differ significantly from the actual measurements at $\omega = 0$.) The values of B_1 are shown as a function of temperature in Fig. 5. The data are in good agreement with other data in the literature, and also have sufficient precision to show the effect of second-sound frequency. In all cases the values determined with the 20 modes (square symbols) are higher than the values determined with the 10 modes (circles). The differences between the two measurements at each temperature taken with the 3.81-cm resonator are shown in Fig. 6. The scatter is large since ΔB_1 is only on the order of 2% of B_1. The smooth curve is the prediction of the Hall-Vinen theory.[30] Values of B_1 at 1.65 K are shown as a function of the second sound frequency in Fig. 7. Measurements were taken with the 10 and 20 modes of the 3.81-cm resonator,

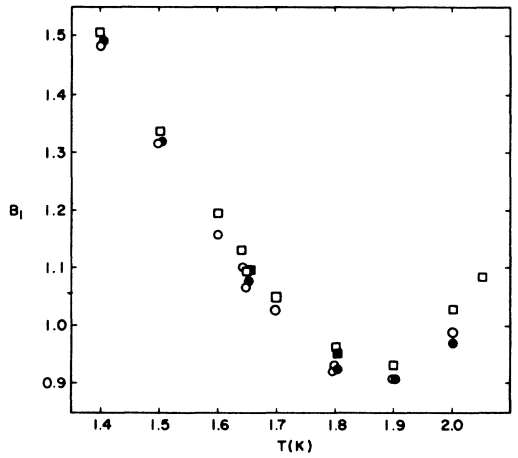

FIG. 5. Mutual friction parameter B_1 vs T. The parameters were determined from measurements of resonance linewidths $\gamma(\omega)$ as described in the text. The various symbols correspond to different resonators and modes, as stated in the caption to Fig. 3. The frequencies of the 20 modes (squares) are a factor 1.831 higher than the frequencies of the 10 modes (circles); correspondingly, B_1 is always higher for the 20 modes.

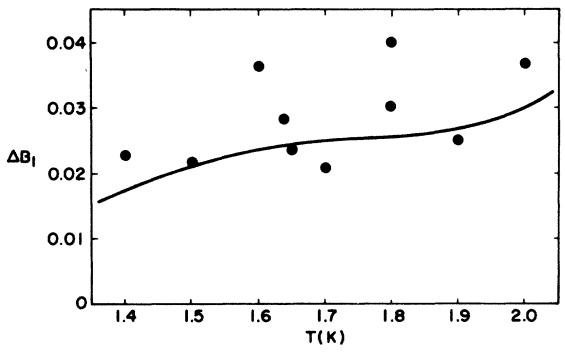

FIG. 6. Difference between the B_1 values for the 20 and 10 modes of the 3.81-cm resonator, vs T. The smooth curve is the prediction of the Hall-Vinen theory.

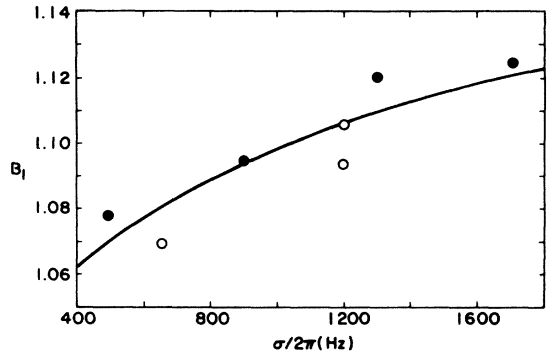

FIG. 7. Mutual friction parameter B_1 vs second-sound frequency $\sigma_0/2\pi$ at 1.65 K. The open and closed symbols correspond to data taken with the 3.81- and 5.08-cm resonators, respectively. The smooth curve is the prediction of the Hall-Vinen theory.

and the 10, 20, 30, and 40 modes of the 5.08-cm resonator. The smooth curve is the prediction of the Hall-Vinen theory.[30] Given the large scatter in Figs. 6 and 7, the agreement with the Hall-Vinen theory is satisfactory.

IX. SUMMARY AND CONCLUDING REMARKS

The dependence of the velocity of second sound in helium II on the rate of rotation has been measured. The results are in close agreements with the calculations of Mehl,[22] which were based on the Hall-Vinen theory of mutual friction. Experimental values of the mutual friction parameter B_2 were determined from the Δu_2 data. These were found to agree closely with values calculated by Mehl[22] from experimental values of the parameters B_1 and B_1'. The calculation of B_2 involves no free parameters. Stated in another way, the two temperature-dependent scattering parameters (D,D') are capable of fitting three experimental parameters (B_1,B_1',B_2). This agreement between theory and experiment provides new support for the internal consistency and detailed correctness of the Hall-Vinen theory.

The B_2 term arises because of phase effects in the roton-drift-velocity perturbation [Eqs. (3) and (4)]. The same perturbation gives rise to a dependence of all the mutual friction parameters on the second sound frequency. Measurements of the dependence of the parameter B_1 on frequency are reported here for the first time. The measured dependence is in satisfactory agreement with the prediction of the Hall-Vinen theory. This agreement also provides new support for the detailed correctness of the theory.

Measurements of B_1 and B_2 were made in the temperature range 1.4–2.05 K. The rapid dependence of u_2 on temperatures near T_λ made measurements of B_2 above 2.05 K difficult. However, owing to the rapid dependence of all the mutual friction parameters on temperature near T_λ, measurements in this temperature range would be worthwhile, particularly since the critical behavior of B_1 and B_1' has recently been determined.[15] Such measurements should be possible with a redesigned apparatus.

ACKNOWLEDGMENTS

The authors gratefully acknowledge the support of the NSF through Grant No. DMR 72-00184 A01. One of the authors (J.B.M.) expresses his gratitude to Professor F. Pobell for his hospitality at the Kernforschungsanlage, Jülich, Germany, where the final version of this paper was prepared.

[1]H. E. Hall and W. F. Vinen, Proc. R. Soc. Lond. A 238, 204(1956); 238, 215 (1956).
[2]E. M. Lifshitz and L. P. Pitaevskii, Zh. Eksp. Teor. Fiz. 33, 535 (1957), [Sov. Phys.-JETP 6, 418 (1958)].
[3]C. C. Lin, *Liquid Helium: Proceedings of the Enrico Fermi International School of Physics, Course 21* (Academic, New York, 1963), p. 120.
[4]S. V. Iordanskii, Ann. Phys. (N.Y.) 29, 335 (1964); Zh. Eksp. Teor. Fiz. 49, 225 (1966) [Sov. Phys.-JETP 22, 160 (1966)].
[5]H. E. Hall, J. Phys. C 3, 1166 (1970).
[6]S. E. Goodman, Phys. Fluids 14, 1293 (1971).
[7]A. J. Hillel, H. E. Hall, and P. Lucas, J. Phys. C 7, 3341 (1974).
[8]H. A. Snyder, Phys. Fluids 6, 755 (1963).
[9]H. A. Snyder and D. M. Linekin, Phys. Rev. 147, 131 (1966).
[10]H. A. Snyder and Z. Putney, Phys. Rev. 150, 110 (1966).
[11]P. Bendt, Phys. Rev. 153, 280 (1967).
[12]J. A. Lipa, C. J. Pearce, and P. D. Jaman, Phys. Rev. 155, 75 (1967).
[13]P. Lucas, J. Phys. C 3, 1180 (1970).
[14]P. Lucas, J. Phys. C 6, 3372 (1973).
[15]P. Mathieu, A. Serra, and Y. Simon, Phys. Rev. B 14, 3753 (1976).
[16]F. Vidal, M. leRay, and M. Francois, Phys. Lett. A 36, 401 (1971).
[17]F. Vidal, M. leRay, M. Francois, and D. Lhuillier, *Proceedings of the Thirteenth International Conference on Low Temperature Physics* (Plenum, New York, 1974), Vol. 1, pp. 324–327. In this paper the decrease of u_2 in rotation is shown as a quantity ν/Ω, where Ω is the angular velocity and $\nu \propto \Delta u_2/\alpha'$, thus $\nu/\Omega \propto \Delta u_2/\Omega^2$.
[18]F. Vidal and D. Lhuillier, Phys. Rev. B 13, 148 (1976).

[19]I. H. Lynall and J. B. Mehl, Phys. Lett. A 46, 115 (1973).
[20]D. Lhuillier, F. Vidal, M. Francois, and M. leRay, Phys. Lett. A 38, 161 (1972).
[21]D. Lhuillier, C. R. Acad. Sci (Paris) B 275, 61 (1972); F. Vidal, *ibid.* 277, 675 (1973); 277, 723 (1973); D. Lhuillier and F. Vidal, J. Phys. C 7, L254 (1974).
[22]J. B. Mehl, Phys. Rev. B 10, 601 (1974).
[23]R. J. Miller, M. S. thesis (University of Delaware, 1975) (unpublished).
[24]Himmelstein MCRT 2-04, S. Himmelstein & Co., Elk Grove Village, Ill.
[25]Graham Transmiscions Inc., Menomonee Fall, Wisc.
[26]Aquadag, Acheson Colloids Co., Fort Huron, Mich.
[27]HP Model 3320B, Hewlett-Packard Co., Loveland, Colo.
[28]J. Heiserman, J. P. Hulin, J. Maynard, and I. Rudnick, Phys. Rev. B 14, 3862 (1976). The $u_2(p,T)$ data is tabulated in J. Maynard, *ibid.* 14, 3868 (1976).
[29]See, e.g., H. B. Callen, *Thermodynamics* (Wiley, New York, 1960), Chap. 16.
[30]The formalism of Ref. 22 was followed in these calculations. Smoothed values of B_1 from the present work, and of B_1' from Ref. 13 were used to calculate the parameters (D,D') in Eq. (1); these parameters were used in turn to calculate the dependence of B_1 on frequency.